Raman signature to identify the structural transition of single-wall carbon nanotubes under high pressure

Mingguang Yao,[1] Zhigang Wang,[2,3,4] Bingbing Liu,[1,*] Yonggang Zou,[1] Shidan Yu,[1] Wang Lin,[1] Yuanyuan Hou,[1] Shoufu Pan,[2,3] Mingxing Jin,[2] Bo Zou,[1] Tian Cui,[1] Guangtian Zou,[1] and B. Sundqvist[5]

[1]*State Key Laboratory of Superhard Materials, Jilin University, Changchun 130012, China*

[2]*Institute of Atomic and Molecular Physics, Jilin University, Changchun 130012, China*

[3]*State Key Laboratory of Theoretical and Computational Chemistry, Institute of Theoretical Chemistry, Jilin University, Changchun 130023, China*

[4]*Shanghai Institute of Applied Physics, Chinese Academy of Sciences, P.O. Box 800-204, Shanghai 201800, China*

[5]*Department of Physics, Umeå University, 90187 Umeå, Sweden*

(Received 5 April 2007; revised manuscript received 28 August 2008; published 10 November 2008)

Raman spectra of single-walled carbon nanotubes (SWNTs) with diameters of 0.6–1.3 nm have been studied under high pressure. A "plateau" in the pressure dependence of the *G*-band frequencies was observed in all experiments, both with and without pressure transmission medium. Near the onset of the *G*-band plateau, the corresponding radial breathing mode (RBM) lines become very weak. A strong broadening of the full width at half maximum of the RBMs just before the onset of the *G*-band plateau suggests that a structural transition starts in the SWNTs. Raman spectra from SWNTs released from different pressures also indicate that a significant structural transition occurs during the *G*-band plateau process. Simulations of the structural changes and the corresponding Raman modes of a nanotube under compression show a behavior similar to the experimental observations. Based on the experimental results and the theoretical simulation, a detailed model is suggested for the structural transition of SWNTs, corresponding to the experimentally obtained Raman results in the high-pressure domain.

DOI: 10.1103/PhysRevB.78.205411 PACS number(s): 61.48.De, 62.50.−p, 31.15.−p, 78.30.−j

I. INTRODUCTION

Single-wall carbon nanotubes (SWNTs) have been intensively studied for their interesting one-dimensional (1D) physical properties and for their potential applications.[1,2] The physical properties of SWNTs are very sensitive to their geometrical structures and thus can be tuned by an applied pressure.[3] Extensive efforts have been made to understand high-pressure-induced structural evolution of SWNTS using experimental methods such as Raman spectroscopy,[4–12] x-ray diffraction[13,14] and neutron[15] diffraction, and theoretical methods including both molecular-dynamic simulations[16–18] and first-principles calculations.[19] It has been suggested that a structural transition occurs at high pressure, during which the nanotube cross section changes from circular to elliptical then to a peanut shape.[5,7,16–20] Raman spectroscopy is one of the most powerful techniques to study the high-pressure evolution of SWNTs,[21] and the most characteristic vibrational modes are the radial breathing mode (RBM) and the tangential modes (*G* band). A number of studies have reported the disappearance of RBMs from the spectrum above a critical pressure (about 2 GPa in most cases), and this is interpreted as the signature of a structural transition occurring near this pressure.[7,9] However, later studies found that the RBMs do not disappear even at 10 GPa.[4] The vanishing of the RBM thus cannot be considered as a sign of a structural phase transition. Very recently, Yang *et al.*[16] predicted that the frequencies of the RBMs undergo an abrupt change at the structural transition of SWNTs and that the RBMs can exist above the critical pressure. The "transformation" signature of the RBM modes is thus still debated. On the other hand, a slope change or a characteristic plateau in the pressure dependence of the *G*-band frequencies after the disappearance of RBMs is also found in several studies.[8–10] This has been related either to a structural transition or to adsorption of the pressure transmission medium (PTM) molecules around nanotubes. Therefore, it is necessary to investigate further whether there is actually any fingerprint signature in the Raman spectrum that can be used to identify a structural transition and preferably also how the structure transforms at the critical pressure. We have therefore carried out Raman measurements on the SWNT samples with a wide diameter distribution under high pressure and tried to correlate the experimental results with the results of theoretical calculations of structure-induced change in Raman spectrum under compression.

In this work, we studied the SWNTs with a wide diameter distribution (~0.6–1.3 nm) and a near IR laser (830 nm) was used to excite this sample which produces a strong Raman signal and gives us the possibility to study simultaneously the progressive structural changes in nanotubes with many different diameters under elevated pressures. As in several earlier studies we found that a plateau occurs for the *G*-band under high pressure, but unlike what is observed in previous studies RBMs can still be detected even up to 14 GPa and their frequencies increase almost linearly, without an abrupt change, throughout the plateau of the *G* band. Based on an analysis of the linewidth of the RBM versus pressure, a structural transition in the SWNT was suggested to start before the onset of the *G*-band plateau. Furthermore, our Raman results for SWNTs released from different pressure domains indicate that a significant structural transition occurs during the *G*-band plateau process. In addition to this experimental work we performed a theoretical calculation

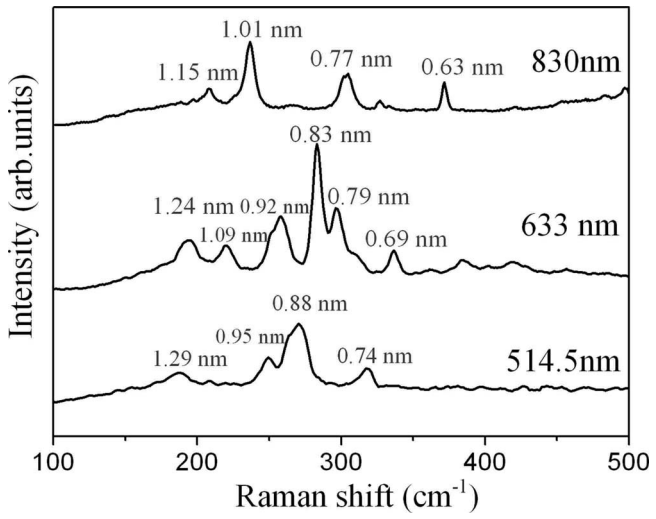

FIG. 1. RBMs of the nanotubes measured using three excitation wavelengths of 514.5, 632.8, and 830 nm. For each RBM peak the corresponding diameter (in nanometers) is indicated.

using the density-functional theory (DFT), which also yields the frequencies of the Raman modes as functions of the structural evolution. Based on both the experimental results and the theoretical simulation, a detailed model of the structural transition in SWNTs under high pressure is suggested.

II. EXPERIMENTAL DETAILS

The SWNTs used in this study were purchased from South West Nanotechnology, Inc. (USA) and were produced by the high-pressure catalytic decomposition of carbon monoxide (HiPco process). The SWNTs were purified according to the product instruction of company and were used in our studies without any further treatment. Our transmission electron microscopy (TEM) observations show that the SWNTs mostly form bundles and that a part of the nanotubes is open. Raman spectroscopy equipped with three excitation wavelengths (514.5, 632.8, and 830 nm) is further employed to characterize the SWNT sample. The Raman measurements show that the sample is homogeneous and the typical Raman spectra of the nanotubes are shown in Fig. 1. On the spectra we show one of the most characteristic regions of the Raman spectra of SWNTs: the low-energy RBMs, for which it is well known that the frequency ω (cm^{-1}) is inversely proportional to the tube diameter d (in nanometers),[22] $d=224/(\omega-14)$. Thus, as shown in Fig. 1, the diameter distribution of the SWNTs excited was calculated to be in the range of 0.6–1.3 nm.

The high pressure Raman experiments up to 30 GPa were carried out either with or without a pressure transmission medium. In the experiments using PTM, a small piece of SWNTs samples, a ruby chip for pressure calibration, and the PTM were loaded in a hole of ~75–100 μm diameter drilled in a preindented (~100 um) steel gasket of a Mao-Bell-type diamond-anvil cell. The PTMs used here are either the standard 4:1 methanol to ethanol mixture or liquid argon. In the experiments without PTM, the gasket hole was filled by approximately half and then a tiny ruby chip for pressure calibration was loaded. More sample material was then added and manually pressed until the gasket hole was fully filled.

In the high-pressure measurements, we excited the Raman spectra with both an 830 nm IR laser, a 514.5 nm (argon ion) laser, and a 633 nm (He-Ne) laser in order to compare the results for nanotubes with different chiralities and diameters. All Raman-scattering experiments were carried out at room temperature using a spectrometer (Renishaw inVia, UK) with double-notch filtering and an air-cooled charge-coupled device (CCD) detector. A 50× long focal length microscope objective was used to focus the beam on the sample and the laser beam size was approximately 1 μm inside the high-pressure cell. According to the specifications of the manufacturer, the spectral resolution of the Raman system was ~1 cm^{-1} or better for all the lasers.

III. EXPERIMENTAL RESULTS

Figure 2(a) shows the Raman spectra of the SWNTs measured with 830 nm laser excitation under high pressure to 22.1 GPa. In this experiment, liquid argon was used as PTM, but very similar results were also obtained using the methanol/ethanol mixture. We can see that both the G band and the RBM signals become weaker and broader with increasing pressure. Because of these effects it becomes increasingly difficult to fit each component of the G band accurately by Lorentzian components at higher pressures. The only feature that can be plotted with good accuracy at all pressures is the position of the most intense peak of the G band. The same problem was also reported by Merlen *et al.*[4] The positions of the most intense peak in the G band (originally at 1594 cm^{-1}) and of the RBMs are plotted as functions of pressure in Fig. 2(b), while the pressure dependence of the intensity of the RBMs is plotted in Fig. 2(c). For the G band, we observed an initial blueshift of 7.8 ± 0.2 cm^{-1}/GPa with pressure. The pressure slope changes near 8 GPa, and a plateau with almost constant phonon frequency is formed in the range from ~8 to 15 GPa for increasing pressure. For the RBMs, a linear blueshift with increasing pressure is observed up to 14 GPa, even throughout the G-band plateau range. Unlike the pressure dependence of the frequency, it should be noted [Fig. 2(c)] that the intensity of the RBM peak at 236 cm^{-1} decreases almost linearly with increasing pressure up to ~7.5 GPa. Above this pressure the intensity becomes very low but still detectable and decreases only very slowly with further increases in pressure. The intensity of the RBM peak at 302 cm^{-1} also decreases almost linearly, but with a different slope, up to ~9.5 GPa, then becomes weak and almost independent of pressure in the same way. In both cases, the pressures where the slope is found to change agree well with the onset of the plateau in the G-band data in Fig. 2(b), considering the scatter in the data. To compare the intensity changes for the RBMs and the G band during the pressure increase, the original Raman spectra at 0.87, 8.51, and 11.65 GPa are shown in Fig. 2(d). It is obvious that the intensities of the lowest-frequency RBM has decreased more than that of the G band (and high-frequency RBMs) when

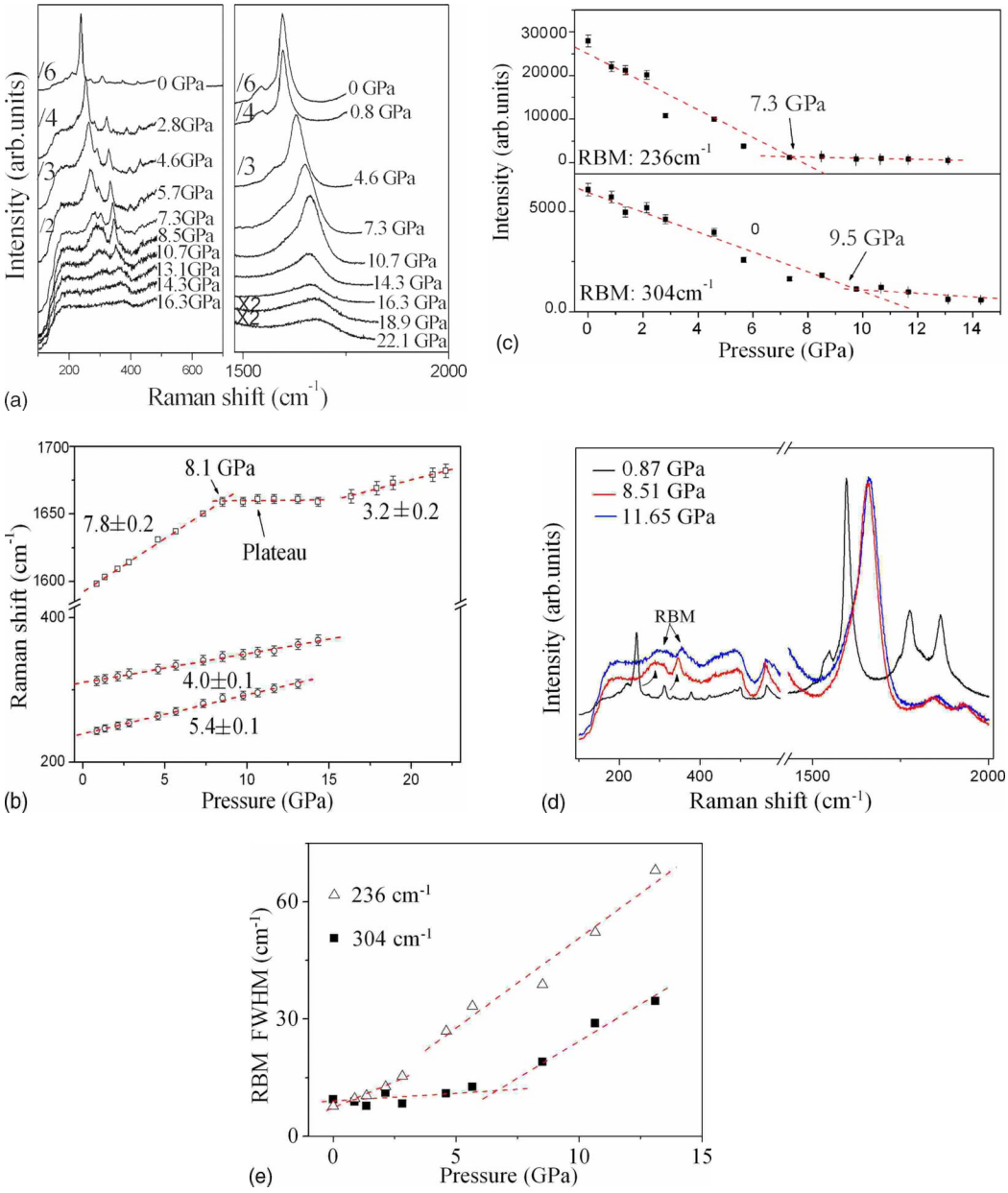

FIG. 2. (Color online) (a) Raman spectra in the RBM and *G*-band regions for SWNTs, measured with 830 nm laser excitation using liquid argon as PTM. (b) The frequencies of two RBMs (circles) and the most intense *G*-band peak (squares) near 1594 cm^{-1} as a function of pressure. (c) The intensities of the two dominant RBMs as functions of pressure. (d) Raman spectra of SWNTs at 0.87, 8.51, and 11.65 GPa, *G*-band intensity is normalized. (e) The linewidths of the two dominant RBMs (at 236 and 304 cm^{-1}) as functions of pressure.

the sample is submitted to pressures near the onset of the plateau (8.51 GPa) or in the plateau region (11.65 GPa). Thus we can say that near the onset pressure of the *G*-band plateau, the low-frequency RBM intensities decreases strongly and these modes become very weak. (Note that we do not observe a complete vanishing of the RBM.) We further plot the full width at half maximum (FWHM) of the two dominant RBMs as functions of pressure in Fig. 2(e). As suggested in a very recent work, the FWHM of RBM can be used as the signature of the first structural transition of SWNTs under high pressure.[12] We observe that there is an obvious change in the slope of the RBM linewidth versus pressure for the 236 cm^{-1} peak at ~4 GPa, while the corresponding onset of an increased linewidth for the 304 cm^{-1} peak is at ~6.5 GPa. Both pressures are lower than that for the onset of the *G*-band plateau. This result will be discussed further below together with other results indicating a possible initial structural modification of the SWNT cross section from circular to elliptic.

It has been suggested in several papers that the interactions between the PTM and the sample have strong effects on the Raman anomalies observed.[8,9] To study the influence of the PTM on the Raman behavior of SWNTs under high pressure and to find out if the observed phenomena depend on the PTM, we also performed experiments without such a medium. Raman spectra from such an experiment are shown

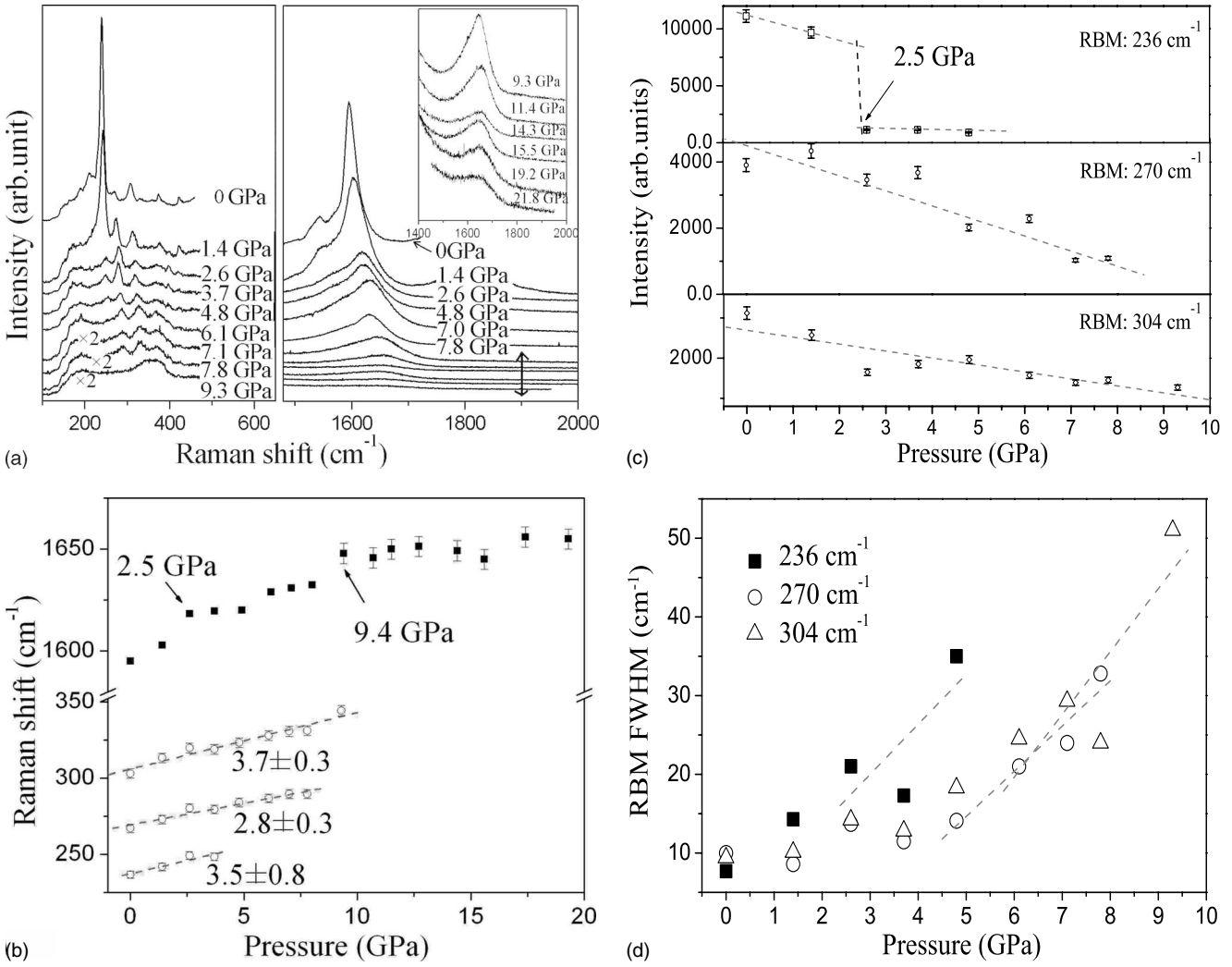

FIG. 3. (a) The Raman spectra of SWNTs measured with 830 nm laser excitation without PTM. (b) The frequencies of RBMs (circle) and the *G* band (square) (originally at 1594 cm^{-1}) as functions of pressure. (c) The intensities of three dominant RBMs (236, 270, and 304 cm^{-1}) as a functions of pressure. (d) The linewidths of three RBMs (at 236, 270, and 304 cm^{-1}) as functions of pressure.

in Fig. 3. We can clearly see several steps or plateaus for the *G*-band frequency, and the intensity of the RBM peaks drops significantly at pressures correlated with the onsets of these plateaus. For example, the *G*-band shows a plateau at ~2.5 GPa where the intensity of the RBM peak at 236 cm^{-1} drops sharply to become very weak. Another obvious plateau occurs at ~10 GPa where the two RBM peaks at 270 and 304 cm^{-1} have decreased to extremely low levels. As shown in Fig. 3(d), the FWHM for the RBM peak at 236 cm^{-1} increases with increasing pressure already from the start of the experiment, while for the peaks at 270 and 304 cm^{-1} the linewidth begins to increase at 4–5 GPa. In some cases, we observed that the slope of the *G*-band shift changed strongly without showing a horizontal plateau at pressures where the RBMs dropped rapidly in intensity. Note that the frequencies of most RBMs increase almost linearly to 10 GPa without any obvious change in slope. In addition, the results also indicate that the plateau behavior of the *G* band is not related to the adsorption of molecular species from the PTM on to the surface of SWNTs since it appears also without a PTM. This rules out one of the possible reasons mentioned in Sec. I.

To further confirm the above observation, we have measured the Raman spectra of SWNTs by using an excitation wavelength of 514.5 nm. This laser wavelength excites nanotubes with a dominant diameter distribution in the range of 0.95–0.74 nm, different from those excited by the 830 nm radiation (mainly 1.01–0.63 nm). Figure 4 shows the frequency of the *G* band as a function of applied pressure and the inset shows the intensity change of the RBMs with increasing pressure. In the experiments with a PTM (methanol/ethanol mixture) this mode indicates a transition near ~12 GPa. The corresponding intensities of the RBMs for the dominating nanotubes (270 and 318 cm^{-1}) decrease gradually and become too weak to be detected beyond ~10 GPa, which is close to the onset of the plateau. Further, the FWHM of the dominant RBMs as a function of pressure shows an obvious change in the slope in the pressure variation of the RBM linewidth, having a similar tendency with the Raman results from 830 nm laser. We can see that the

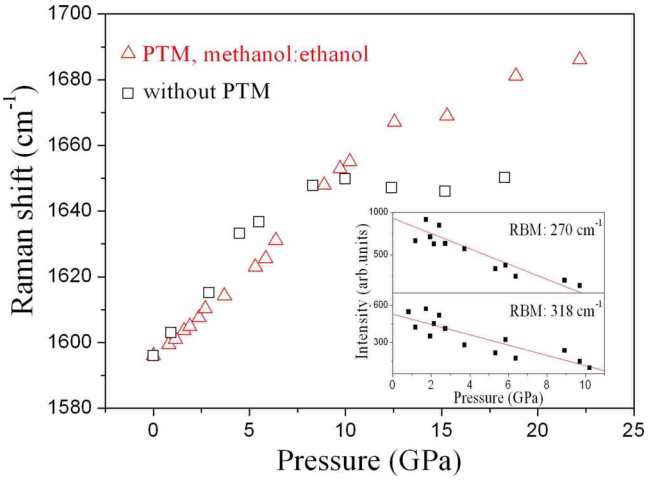

FIG. 4. (Color online) The frequency of the G band (1594 cm^{-1} mode) as a function of applied pressure with a PTM (triangles) or without a PTM (squares); inset shows the intensity change in the dominant RBMs with increasing pressure (using a PTM). The excitation wavelength is 514.5 nm.

plateau is also present in the experiments without a PTM, and that the plateau starts at a lower pressure (~7.5 GPa) than in the experiments using a PTM.

Finally, we also carried out experiments without a PTM using a 633 nm laser and found that in this case the onset of the plateau can be at ~4, ~6, or ~8 GPa, respectively, depending on the exact nonhydrostatic pressure conditions in different runs. In these cases, the intensity of the corresponding RBMs again decreased gradually to become very weak near the onset pressure of the plateau.

In order to investigate whether any permanent structural deformation of the SWNTs is induced during the plateau stage we also measured the ambient-condition Raman spectra of carbon nanotubes released from different pressures using 830 and 633 nm laser excitations. The results are shown in Figs. 5(a) and 5(b). After unloading the SWNTs from the middle of the plateau at ~12.8 GPa in the experiment with a PTM using the 830 nm laser, the Raman spectrum is similar to that of as-grown SWNTs, indicating that no obvious irreversible structural transition occurs in SWNTs [Fig. 5(a)]. However, after unloading the SWNTs from pressures higher than the upper limit of the plateau, i.e., from 22.1 or 31.3 GPa, the intensity of the disorder-induced D band increases and those of the RBMs decrease significantly, indicating that some permanent damage or deformation was imposed on the SWNTs. In the experiments without a PTM [Fig. 5(b)], unloading SWNTs from 4 GPa [within the first small plateau in Fig. 3(b)], the RBM peaks at 193 and 219 cm^{-1} decrease to become very weak, indicating that large diameter nanotubes have suffered severe deformation. Unloading SWNTs from 16 GPa, where another plateau occurs [see Fig. 3(b)], all the RBM peaks became very weak and the ratio between the D and G peaks became high, indicating that important transformations occurred. It thus seems quite probable that some structural transition occurs in SWNTs during the plateau process.

Comparing the Raman results from the experiments using argon or methanol/ethanol mixture as PTM with those from

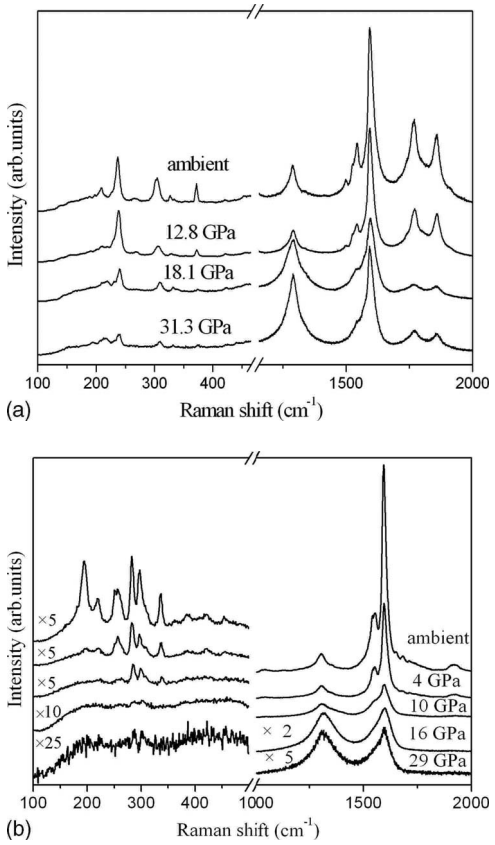

FIG. 5. The Raman spectra of SWNTs released from different pressure (a) in the experiments with a PTM, measured with 830 nm laser excitation, and (b) in the experiments without a PTM, measured with 633 nm laser excitation.

the experiments without a PTM, it is clear that a plateau or a sudden change in slope in the G-band energy versus pressure appears in all cases. During the G-band plateau process, the RBM frequency can shift up linearly with pressure even throughout the plateau, but the intensity is always very weak or even too weak to be experimentally detected. Therefore it is believed that this phenomenon is an intrinsic feature of SWNTs and is related to a structural transition near the onset pressure of the plateau. In the plateau, the G-band frequency shift changes relatively less than that of RBM. In fact, such an effect has been observed by another method without using high pressure. Zhang *et al.*[23] found that a relatively larger change $\Delta\omega_{\mathrm{RBM}}$ in the RBMs and a relatively smaller change $\Delta\omega_G$ in the G band is induced by the presence of a substrate, and this effect is attributed to radial deformation of the SWNTs. Actually, this phenomenon was also observed in an experiment on isolated nanotubes but not discussed in detail.[9] The Raman behavior of individual nanotubes under high pressure thus shows a tendency similar to that of bundled ones. To understand the intrinsic character of SWNTs under high pressure, it is thus feasible to study the Raman behavior of an isolated nanotube under pressure by theoretical simulations.

IV. THEORETICAL SIMULATIONS

To understand our experimental results, we have performed numerical simulations to explore the effect of a nano-

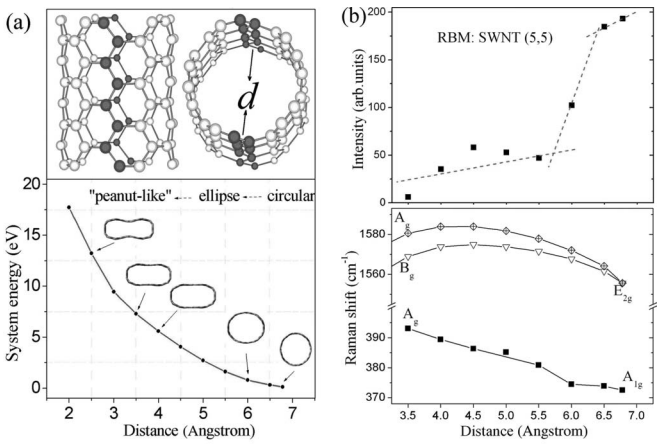

FIG. 6. (a) Sketch of a (5,5) FSWNT model (upper panel), and the system energies of deformed nanotubes with different optimized structural shapes. The distance (x axis) is the shortest distance between two C atoms located opposite each other on different sides of the axis of the FSWNT (marked with black atoms). (b) Calculated relative intensities and Raman shifts for the same nanotube.

tube structural transition on the Raman spectra of SWNTs. In the simulations, the structural changes in the chosen nanotube model and the frequencies of the corresponding Raman modes under compression were calculated from first principles using the local-density approximation (LDA) in density-functional theory. The relationship between force constant K and frequency ω is described as

$$\omega \sim \sqrt{k/m}.$$

The computation was carried out using the GAUSSIAN 03 program package.[24]

As we know, the external force field (high pressure) acting on the SWNT, which induces the deformation of the SWNT, will not play a role on the Hamiltonian of the electronic Schrödinger equation but only has an effect on controlling the coordinates of the atoms on the nanotube. On the other hand, since the C-C bond is strong and carbon nanotubes show extraordinarily high stiffness and strength in the axial direction, the axial deformation under moderate pressure can be largely ignored while substantial radial deformation is already induced.[13] Such approximation of only considering the radial deformation of SWNTs to study the properties of SWNTs under high pressure gives a quite similar result comparing to other theoretical simulations.[25] Thus, to approximately simulate the structural transition of SWNTs under high pressure, only the radial deformation is taken into account in this work. For simplicity, we have constructed a (5,5) single-wall carbon nanotube model with finite length (FSWNT). We first shorten the distance d (*equal to the diameter of nanotube*) between the two opposite lines of carbon atoms on the nanotube, as marked with black color in our FSWNT [see Fig. 6(a)], by 0.5 Å/step, and then optimize the structure to simulate the structural change in SWNT under compression. In brief, we first control the distance d between the two opposite lines of carbon atoms on the nanotube and then perform full optimizations on the other carbon atoms to optimize the system structure. This so-called "partial optimization" method for the geometry optimization has also been used in some other systems.[26,27] For such a large system, containing 80 C atoms, we optimize the structure and calculate the vibrational frequency using the double-ζ basis.[28] Further, one d-polarization function for each C atom is added to improve the results [marked with 3-21G(d)]. The optimized structures are shown in Fig. 6. We can see that the cross section of the optimized SWNT changes from circular to elliptical and to a peanut-shaped structure, in good agreement with simulations by others, when applying high pressure.[19] The Raman spectra for the optimized FSWNT structure were calculated according to the method used in Ref. 29. From the calculated Raman spectra, we can obtain the frequency of RBM and G band, as well as the intensity of RBM. A RBM frequency (A_{1g}) of 373 cm^{-1} and a E_{2g} mode in the G band at 1556 cm^{-1} were obtained for the (5,5) FSWNT with D_{5d} symmetry at ambient condition, which is consistent with other theoretical calculations.[19] The intensity and frequency of the RBM and the frequency of the G mode are plotted in Fig. 6(b) as functions of the distance d. The frequency of the G mode first increases and then becomes almost constant, followed by even a slight decrease when shortening the distance, and the intensity of the RBM noticeably drops almost simultaneously and then becomes weak while the frequency of the RBM increases monotonously. It is noted that the RBM mode can still exist until the peanut structure forms.

V. DISCUSSION

In the simulation, the general tendencies of the frequency shift of the G band and the RBM with the structural changes are in good qualitative agreement with our experimental observations under pressure. This indicates that the anomalous G-band frequency shift (the plateaus observed in our experiments) can originate from a structural change in the SWNTs under pressure. In two very recent reports, both Yang *et al.*[18] and Cailler *et al.*[12] also suggested that the anomalous plateau behavior of the G band possibly indicates a structural transition in the SWNTs under pressure. In these reports, however, the detailed structural change in nanotubes is still not clear. On the other hand, based on our Raman results on the SWNTs released from high pressure, we know that some structural transitions (or deformations) occur in carbon nanotubes during the G-band plateau process. Actually, in an early work, Sharma *et al.*[14] also suggested a structural change in SWNTs at 10 GPa based on an *in situ* x-ray diffraction study of SWNTs under pressure, and Teredesai *et al.*[10] reported the onset of a G-band plateau when they make high-pressure Raman experiments on a similar SWNT sample, though the real structural transition is unclear. All these results indicate that a structural transition is induced near the onset of the G-band plateau. As demonstrated in our simulation, this structural transition involves a change of cross section from circular to an ellipselike shape and then to a flattened oval shape. In addition, our simulations also indicate a significant decrease in the RBM intensity at the onset of a G-band plateau. In theory, Yang *et al.*[16] also predicted

that the RBM intensity will decrease significantly or even become too weak to be experimentally detected at the nanotube structural transition. In our experiments, we do observe that the intensity of the RBM always decreases (by an abrupt drop or by a gradual decrease) to become weak (or to disappear, in some cases) near the onset of the *G*-band plateau.

According to group theory analysis, we can understand the behavior of SWNTs during compression. The A_{1g} (RBM) and E_{2g} (G) modes in D_{5d} symmetry will transform into the modes in the C_{2h} symmetry: $A_{1g} \rightarrow A_g$ and $E_{2g} \rightarrow A_g + B_g$, where A_g and B_g preserve the vibrational characteristic of the E_{2g} tangential modes perpendicular to the tube axis and the direction of pressure. When compression acts on the FSWNT along the radial direction, this will result in an increase in the vibrational force constant for the Ag mode, and thus the frequency of the Ag mode increases. The E_{2g} mode is associated with the out-of-phase vibrations of adjacent carbon atoms parallel to the surface of the tube and is sensitive to the state of the C-C bonds parallel to the tube. As the radial deformation evolves, the C-C bond length in the middle of the optimized deformed FSWNT first shortens and then elongates, corresponding to the increase and then decrease in the frequency of the E_{2g} mode.

It is worth noting that, in our simulations, the anomalous frequency shift of the *G* band correlated with the structural change does not take place as soon as the initiation of the structural transition of SWNT but in a critical structural transition domain (from an ellipselike shape to a flattened oval shape). This is also consistent with our experimental results. As stated by Caillier *et al.*,[12] the obvious change in the slope of the FWHM versus pressure curves can be assumed to be the signature of the start of a structural transition in the nanotube (the nanotube cross section changes without involving an important volume reduction). In our experiments, the pressure where the FWHM begins to increase is always lower than that of the onset of the *G*-band plateau, indicating that the structural change in the nanotubes starts (e.g., by a slight structural modification) well before the critical structural transition domain (corresponding to the *G*-band plateau). This is consistent with our simulations. In addition, the pressure where the FWHM begins to increase with increasing pressure is found to depend on the nanotube diameter. The larger the nanotube diameter, the lower the pressure for this change to take place; that is to say, larger diameter nanotubes start their structural transition at lower pressures. This tendency is consistent with other theoretical predictions, where the critical pressure P_{cr} for the structural transition depends on the tube diameter as $P_{cr} \sim d^{-3}$.[5,30] For example, the change in the FWHM with pressure for the RBM at 304 cm^{-1} ($d \sim 0.8$ nm) starts at 6.5 GPa, which is very close to the theoretically predicted value of ~ 7 GPa.[5] Furthermore, our simulations also show that during the (minor) structural changes in the nanotubes before the *G*-band plateau, the RBM and *G*-band frequencies shift almost linearly with pressure, in good agreement with our and others' experimental results. Therefore, we suggest that the obvious broadening of the FWHM of RBMs at lower pressure indicates an initial minor structural transition of the nanotubes from circular to ellipselike shapes, while the most obvious changes in the Raman data (e.g., the appearance of a *G*-band plateau and the corresponding drop in RBM intensity before the plateau) correspond to the more dramatic change in cross section from an ellipselike shape to a flattened ellipse. Additionally, the good agreement between our simulation and our experimental results also indicate that the radial deformation of SWNTs is dominant when the nanotubes are submitted to moderately high pressures. This is also consistent with the prediction that the nanotube is very stiff in its axial direction but soft in its radial direction.

From the above model, we can also understand the behavior of SWNTs under high pressure above the plateau of the *G* band. As observed in our experiments (see Figs. 2 and 4), the pressure dependence of the *G*-band frequency was close to that of graphite under high pressure in the experiments using a PTM.[31] We interpret these results as evidence supporting a further structural transition in SWNTs at higher pressures, as observed in our simulations. After the structural transition when the SWNT cross section changes from an ellipselike shape to a flattened ellipse, a further increase in pressure possibly leads to a peanut-shaped cross section or even a collapse of the SWNTs into a narrow strip with a double-layer graphene structure. Therefore, the collapsed nanostructures of SWNTs have a high-pressure evolution resembling that of graphite in terms of density and hybridization. The permanent change in the Raman frequencies and modes observed in nanotubes decompressed from different pressures also supports our model. For example, the characteristic *D* band, *G* band, and RBM band of SWNTs unloaded from a pressure (with a PTM) in the middle of the plateau (12.8 GPa) change only slightly, indicating that the structural deformation is almost reversible. This corresponds to a slight deformation of nanotubes during the plateau process, as described in our theoretical simulations. When the nanotubes undergo the *G*-band plateau process, they suffer more significant structural changes which possibly results in some irreversible deformation or even destruction of nanotubes. Such changes are identified in our Raman results on the SWNTs unloaded from a pressure above the plateau process (22.1 GPa), i.e., obvious decreases in the intensities of the RBM and *G* band. The Raman results on SWNTs released from the high-pressure experiments without a PTM also support our suggestion. For each completed plateau, the corresponding nanotubes, which are believed to transform "causing" the plateau, have suffered significant structural changes or even destruction. This model thus enables us to explain all the phenomena observed by Raman scattering from SWNTs under high pressure. To verify if the model is versatile for all kinds of nanotubes, further theoretical simulations should be performed on nanotubes with different diameters and chiralities.

VI. SUMMARY AND CONCLUSIONS

We have studied the Raman spectra of single-walled carbon nanotubes in high-pressure experiments performed with or without a pressure transmission medium. The pressure dependence of the *G*-band frequencies was observed to show a "plateaulike" behavior in all experiments. We observe a clear correlation between the onset pressure of such plateaus

and the points where at least one radial breathing mode peak becomes very weak, sometimes too weak to be experimentally detected, either by an abrupt drop or by a gradual decrease in intensity. Raman measurements on nanotubes released from different pressures show that a significant structural change may occur during the *G*-band "plateau" process. We also carried out theoretical simulations of the structural evolution of a (5,5) nanotube by compressing it and then calculating the corresponding Raman modes of the nanotube with the optimized structure. The results show that when the SWNT cross section changes from a circle to an ellipselike shape and then to a flattened oval shape, the calculated Raman frequencies have a behavior similar to the experimental observations. The change in the FWHM of the RBM peaks further support this image of the structural evolution of SWNTs under high pressure. Based on our simulations and other theoretical predictions, it is suggested that the cross section of nanotubes changes from circular to elliptical before the onset of the *G*-band plateau, which can be observed from the FWHM change in the RBM peaks; near the onset of the *G*-band plateau, further intensity changes in the RBMs are believed to correlate with the start of a structural transition involving a change of cross section from an ellipselike shape to a flattened oval shape. We thus show a possible way to detect, model, and analyze the structural transition of SWNTs under high pressure.

ACKNOWLEDGMENTS

This work was supported financially by the National Natural Science Foundation of China (Grants No. 10674053, No. 10574053, No. 10534010, and No. 10374037), by the Cultivation Fund of the Key Scientific and Technical Innovation Project (Grant No. 2004-295), by the Program for Changjiang Scholar and Innovative Research Team in University (Grant No. IRT0625), by the 2007 Cheung Kong Scholars Programme, by the National Fund for Fostering Talents of Basic Science (Grant No. J0730311) of MOE of China, by the National Basic Research Program of China (Grants No. 2005CB724400 and No. 2001CB711201), by the Project for Scientific and Technical Development of Jilin Province, by Graduate Innovation Laboratory of Jilin University, and also by an exchange grant from the Swedish Research Council through the SIDA-Swedish Research Links exchange program. W.Z.G thanks China Postdoctoral Science Foundation (Grant No. 20070420685) and Shanghai Postdoctoral Scientific Program (Grant No. 07R214159) for support.

*liubb@jlu.edu.cn; comments on the theoretical simulation should be addressed to wangzg@jlu.edu.cn

[1] *Carbon Nanotubes: Synthesis, Structure, Properties and Applications*, edited by M. S. Dresselhaus, G. Dresselhaus, and P. Avouris (Springer, Berlin, 2001).
[2] L. Sun, F. Banhart, A. V. Krasheninnikov, J. A. Rodríguez-Manzo, M. Terrones, and P. M. Ajayan, Science **312**, 1199 (2006).
[3] O. Gülseren, T. Yildirim, S. Ciraci, and Ç. Kiliç, Phys. Rev. B **65**, 155410 (2002).
[4] A. Merlen, N. Bendiab, P. Toulemonde, A. Aouizerat, A. San Miguel, J. L. Sauvajol, G. Montagnac, H. Cardon, and P. Petit, Phys. Rev. B **72**, 035409 (2005).
[5] J. A. Elliott, J. K. W. Sandler, A. H. Windle, R. J. Young, and M. S. P. Shaffer, Phys. Rev. Lett. **92**, 095501 (2004).
[6] U. D. Venkateswaran, A. M. Rao, E. Richter, M. Menon, A. Rinzler, R. E. Smalley, and P. C. Eklund, Phys. Rev. B **59**, 10928 (1999).
[7] M. J. Peters, L. E. McNeil, J. P. Lu, and D. Kahn, Phys. Rev. B **61**, 5939 (2000).
[8] M. S. Amer, M. M. El-Ashry, and J. F. Maguire, J. Chem. Phys. **121**, 2752 (2004).
[9] S. Lebedkin, K. Arnold, O. Kiowski, F. Hennrich, and M. M. Kappes, Phys. Rev. B **73**, 094109 (2006).
[10] P. V. Teredesai, A. K. Sood, D. V. S. Muthu, R. Sen, A. Govindaraj, and C. N. R. Rao, Chem. Phys. Lett. **319**, 296 (2000).
[11] U. D. Venkateswaran, D. L. Masica, G. U. Sumanasekara, C. A. Furtado, U. J. Kim, and P. C. Eklund, Phys. Rev. B **68**, 241406(R) (2003).
[12] Ch. Caillier, D. Machon, A. San-Miguel, R. Arenal, G. Montagnac, H. Cardon, M. Kalbac, M. Zukalova, and L. Kavan, Phys. Rev. B **77**, 125418 (2008).
[13] J. Tang, L.-C. Qin, T. Sasaki, M. Yudasaka, A. Matsushita, and S. Iijima, Phys. Rev. Lett. **85**, 1887 (2000).
[14] S. M. Sharma, S. Karmakar, S. K. Sikka, P. V. Teredesai, A. K. Sood, A. Govindaraj, and C. N. R. Rao, Phys. Rev. B **63**, 205417 (2001).
[15] S. Rols, I. N. Gontcharenko, R. Almairac, J. L. Sauvajol, and I. Mirebeau, Phys. Rev. B **64**, 153401 (2001).
[16] W. Yang, R. Z. Wang, X. M. Song, B. Wang, and H. Yan, Phys. Rev. B **75**, 045425 (2007).
[17] P. Tangney, R. B. Capaz, C. D. Spataru, M. L. Cohen, and S. G. Louie, Nano Lett. **5**, 2268 (2005).
[18] W. Yang, R. Z. Wang, Y. F. Wang, X. M. Song, B. Wang, and H. Yan, Phys. Rev. B **76**, 033402 (2007).
[19] G. Wu, J. Zhou, and J. M. Dong, Phys. Rev. B **72**, 115411 (2005).
[20] S. A. Chesnokov, V. A. Nalimova, A. G. Rinzler, R. E. Smalley, and J. E. Fischer, Phys. Rev. Lett. **82**, 343 (1999).
[21] A. San Miguel, Chem. Soc. Rev. **35**, 876 (2006).
[22] A. M. Rao, J. Chen, E. Richter, U. Schlecht, P. C. Eklund, R. C. Haddon, U. D. Venkateswaran, Y. K. Kwon, and D. Tomanek, Phys. Rev. Lett. **86**, 3895 (2001).
[23] Y. Y. Zhang, J. Zhang, H. B. Son, J. Kong, and Z. F. Liu, J. Am. Chem. Soc. **127**, 17156 (2005).
[24] M. J. Frisch, G. W. Trucks, H. B. Schlegel *et al.*, GAUSSIAN 03, Gaussian, Inc., Pittsburgh, PA, 2003.
[25] M. Hasegawa and K. Nishidate, Phys. Rev. B **74**, 115401 (2006).
[26] A. M. Dokter, M. C. van Hemert, C. M. In't Velt, K. van der Hoef, J. Lugtenburg, H. A. Frank, and E. J. J. Groenen, J. Phys. Chem. A **106**, 9463 (2002).

[27] F. Himo, J. Phys. Chem. A **105**, 7933 (2001).
[28] R. Ditchfield, W. J. Hehre, and J. A. Pople, J. Chem. Phys. **54**, 724 (1971).
[29] X. F. Li, M. D. Sevilla, and L. Sanche, J. Am. Chem. Soc. **125**, 13668 (2003).
[30] J. Zang, A. Treibergs, Y. Han, and F. Liu, Phys. Rev. Lett. **92**, 105501 (2004).
[31] T. L. Schindler and Y. K. Vohra, J. Phys.: Condens. Matter **7**, L637 (1995).